Inorganica Chimica Acta 510 (2020) 119731

Contents lists available at ScienceDirect

Inorganica Chimica Acta

journal homepage: www.elsevier.com/locate/ica

Research paper

Facile synthesis of heterobimetallic [Fe^{II}(μ-diphosphine)Ru^{II}] and homobimetallic [Fe^{II}(μ-diphosphine)Fe^{II}] complexes and their *in vitro* cytotoxic activity on cisplatin-resistant cancer cells

Danya BenYosef[a], Dario Romano[b,c], Mouna Hadiji[d], Paul J. Dyson[d], Burgert Blom[a,*]

[a] Maastricht Science Programme, Faculty of Science and Engineering, Maastricht University, Kapoenstraat 2, PO Box 616, 6200 MD Maastricht, The Netherlands
[b] Department of Biobased Materials, Faculty of Science and Engineering, Maastricht University, Brightlands Chemelot Campus, Urmonderbaan 22, Geleen 6167 RD, The Netherlands
[c] Aachen-Maastricht Institute for Biobased Materials, Brightlands Chemelot Campus, Urmonderbaan 22, Geleen 6167 RD, The Netherlands
[d] Institut des Sciences et Ingénierie Chimiques, Ecole Polytechnique Fédérale de Lausanne (EPFL), CH1015 Lausanne, Switzerland

ARTICLE INFO

Keywords:
Heterobimetallic complexes
Homobimetallic complexes
Anti-cancer activity
μ-Phosphine bridged complexes

ABSTRACT

A series of heterobimetallic [Fe,Ru] and homobimetallic [Fe,Fe] complexes, featuring μ -diphosphine bridges between the two metal centres, are reported along with their *in vitro* cytotoxicity activity on the A2780cisR cell-line. The known starting material [CpFe(CO)$_2$(CH$_3$)] (Cp = η^5-C$_5$H$_5$) **(1)** was reacted with dppe (1,2-bis(diphenylphosphino)ethane) forming the known mononuclear κ^1-dppe complex: [CpFe(CO)(COCH$_3$)(κ^1-dppe)] **(2)** and the known dinuclear complex: and [[CpFe(CO)(COCH$_3$)]$_2$(μ-dppe)] **(3)**. Dimer cleavage reactions between complex **2** and two ruthenium arene complexes [(η^6-*p*-cymene)RuCl$_2$]$_2$ and [(η^6-benzene)RuCl$_2$]$_2$ formed two new heterobimetallic complexes: [CpFe(CO)(COCH$_3$)(μ-dppe)Ru(η^6-cymene)Cl$_2$] **(4)** and [CpFe(CO)(COCH$_3$)(μ-dppe)Ru(η^6-C$_6$H$_6$)Cl$_2$] **(5)**. A homobimetallic system, [[CpFe(CO)(I)]$_2$(μ-dppb)] **(6)** was obtained by the facile reaction between of [CpFe(CO)$_2$I] and 1,4-bis(diphenylphosphino)butane (dppb). Complex **6** was methylated using MeLi to generate the more lipophilic complex [[CpFe(CO)(CH$_3$)]$_2$(μ-dppb)] **(7)**. All of the complexes were fully characterized by spectroscopy (^{1}H, ^{13}C {^{1}H}, ^{31}P {^{1}H} NMR; FTIR, UV–Vis), and high resolution mass spectrometry (HRMS). Density functional theory calculations (DFT) (Level of theory B3LYP, basis set for H, C, P, O, Cl is 6-31 + G(d,p) and for Ru, Fe, I is DGDZVP) on complexes **5** and **6** are also reported. An excellent agreement between the DFT calculated infra-red (IR) spectra of the optimised geometries of **5** and **6** was found with the experimentally determined spectra. *In vitro* cytotoxicity studies of all complexes was carried out on A2780cisR (cisplatin resistant ovarian cancer cell-line) and compared to cisplatin as a positive control and RAPTA-C as a negative control. Although limited to only one cell-line, the results show that the heterobimetallic complexes **4** and **5** are the most cytotoxic (IC_{50} = 4.9 ± 0.4 μM and 6.5 ± 0.1 μM respectively), whilst the dinuclear [Fe,Fe] complexes exhibit no, or very low cytotoxicity.

1. Introduction

In 2020 the WHO estimates the number of new cancer cases to rise to 15 million and currently the disease is responsible for 12% of mortality world-wide [1]. Chemotherapeutic interventions including metal based drugs, are widely employed for treatment [2], to induce cell apopotosis in cancer cells [3,4]. Cisplatin, found to exhibit anticancer properties in the 1960 s by Rosenberg, heralded a new era in cancer chemotherapy [5]. The well-studied mechanism of action of this drug involves impairing cell function by binding to two guanine bases in DNA distorting DNA and inhibiting replication [6–8]. DNA.platinum adducts are recognized by certain proteins which either initiate DNA repair mechanisms, or initiate apoptotic cell death. While cisplatin is a highly effective drug, it causes nephrotoxicity and neurotoxicity and other side effects including hair loss, nausea and vomiting [9]. Other limitations of cisplatin include intrinsic drug resistance or resistance after exposure to some types of tumours, as well as low solubility in aqueous media [10]. Thus, platinum analogues have been developed and studied in order to circumvent these limitations [11–15]. In addition, complexes based on other metals such as gold [16,17], titanium [16], ruthenium [18–28] and iron have also been reported to exhibit anti-cancer properties [9,29–31]. One area that has attracted the

* Corresponding author.
E-mail address: burgert.blom@maastrichtuniversity.nl (B. Blom).

https://doi.org/10.1016/j.ica.2020.119731
Received 30 April 2020; Accepted 1 May 2020
Available online 05 May 2020

attention is the synthesis heterobimetallic systems where potential co-operative behaviour can lead to the potentiation of cytotoxic activity. Systems containing gold(I) and platinum(II) centres, for example, display improved antiproliferative activity, as well as overcome drug resistance issues seen in cisplatin [33]. A study by Fernandez-Gallardo et al. shows that ruthenium-gold heterobimetallic systems reveal higher selectivity and cytotoxicity towards renal and colon cancer cell lines than their mononuclear analogs [34]. Serra et al. elucidated the enhanced redox properties that iron-ruthenium heterobimetallic systems have for catalytic applications, which served as inspiration for our own work [32].

We have focussed on the development of heterobimetallic complexes and explored their use in anti-cancer applications. Our initial focus was arene-ruthenium(II) half-sandwich complexes with one or two trichlorostannyl ligands σ-bound to the Ru(II) centre. The compounds showed poor cytotoxicity due to low solubility in aqueous media, which could be overcome in ionic compounds or by increasing solubility in aqueous media [35,36]. Ruthenium(II) arene complexes bearing a σ -bound germyl group were also prepared and showed low to negligible cytotoxic activity, which was postulated to be due to rapid aquation kinetics [37]. We have also focussed on homo and heterobimetallic systems bearing two group 8 metals and their respective cytotoxcity (Fig. 1). In this regard [Fe,Ru] and [Ru,Ru] complexes bridged with μ-dppm (dppm = 1,1-bis(diphenylphosphino)methane)) were synthesized with the expectation that the presence of iron in the bimetallic compound may increase drug uptake [38a]. The study revealed that a heteronuclear [Fe,Ru] system was indeed substantially more cytotoxic than cisplatin, on A2780 and A2780cisR cell-lines, while a comparable dinuclear [Ru,Ru] system showed a decrease in cytotoxicity.

In the present study, we report on our latest findings in this area, in which we explored the effects of increasing the lipophilicity at the iron centre by replacing the iodo ligand with an acyl group and explored the effect of increasing the spacer length between the Fe and Ru centres to observe changes in cytotoxicity. Studies by Hartinger, for example have shown that spacer length plays a role in cytotoxic action [38e]. Moreover, the preparation and cytotoxic testing of homobimetallic μ-diphosphine [Fe,Fe] complexes is also reported (Fig. 1).

2. Results and discussion

Our strategy to prepare heterobimetallic [Fe,ru] complexes is similar to the one we employed previously [38a], Requiring a suitable mononuclear iron complex, bearing a κ^1 metal bound bisphosphine ligand with a pendant uncoordinated phosphorus atom of the type $L_nFe\leftarrow$:P-P. The pendant uncoordinated phosphine could then, in a second synthetic step, cleave Ru dimer complexes of the type $[RuCl_2(\eta^6$-arene$)]_2$ (arene = benzene and *p*-cymene) [39], to afford the desired dinuclear complexes. We sought complexes bearing a κ^1 dppe (dppe = 1,1-bis(diphenylphosphino)ethane)) ligand, as previously we employed dppm (dppe = 1,1-bis(diphenylphosphino)methane)) [38a], and wanted to increase the spacer length between the Fe and Ru centres. Moreover, we were also interested in obtaining an iron centre which was more lipophilic than in our earlier studies, since we envisioned higher cellular uptake and potential efficacy. A suitable agent for these purposes was the known complex $[CpFe(CO)(COCH_3)(\kappa^1$-dppe$)]$ (Cp = η^5-C_5H_5) (**2**) [42,43]. Complex **2** is accessible *via* a facile migratory insertion route using dppe starting from the known complex $[CpFe(CO)_2(CH_3)]$ **1** [40,41]. Complexes $[CpFe(CO)(COCH_3)(\kappa^1$-dppe$)]$ **2** and $[[CpFe(CO)(COCH_3)]_2(\mu$-dppe$)]$ **3** [44], the latter which exists as a mixture diastereoisomers, are obtained from this reaction (Scheme 1) [42,43]. While compounds **2** and **3** are known, their cytotoxicity has not been determined, and we decided to include them in our *in vitro* cytotoxicity screening studies (see below).

Employing complex **2** as starting material (which is chiral and exists as a mixture of enantiomers: *rac*-**2**) the reaction thereof with the Ru dimer complexes $[RuCl_2(\eta^6$-*p*-cymene$)]_2$ and $[RuCl_2(\eta^6$-$C_6H_6)]_2$ in a 2:1 ratio afforded the heterobimetallic complexes $[CpFe(CO)(COCH_3)(\mu$-dppe$)Ru(\eta^6$*p*-cymene$)Cl_2]$ **4** and $[CpFe(CO)(COCH_3)(\mu$-dppe$)Ru(\eta^6$-$C_6H_6)Cl_2]$ **5**, respectively (Scheme 2) in a straightforward manner. The μ-dppe bridged [Fe,Ru] complexes with no Fe-Ru bond are somewhat rare in the literature [38b–d]. Complex **4** was isolated as a clay red/orange powder in an excellent yield of 85%, while complex **5** required column chromatographic purification using an eluent mixture of 1:1*n*-hexane/ethyl acetate. The latter afforded a light brown powder with a suboptimal yield of 34%. Both complexes exhibit high decomposition temperatures: **4** at 191 °C, and complex **5** at 130 °C.

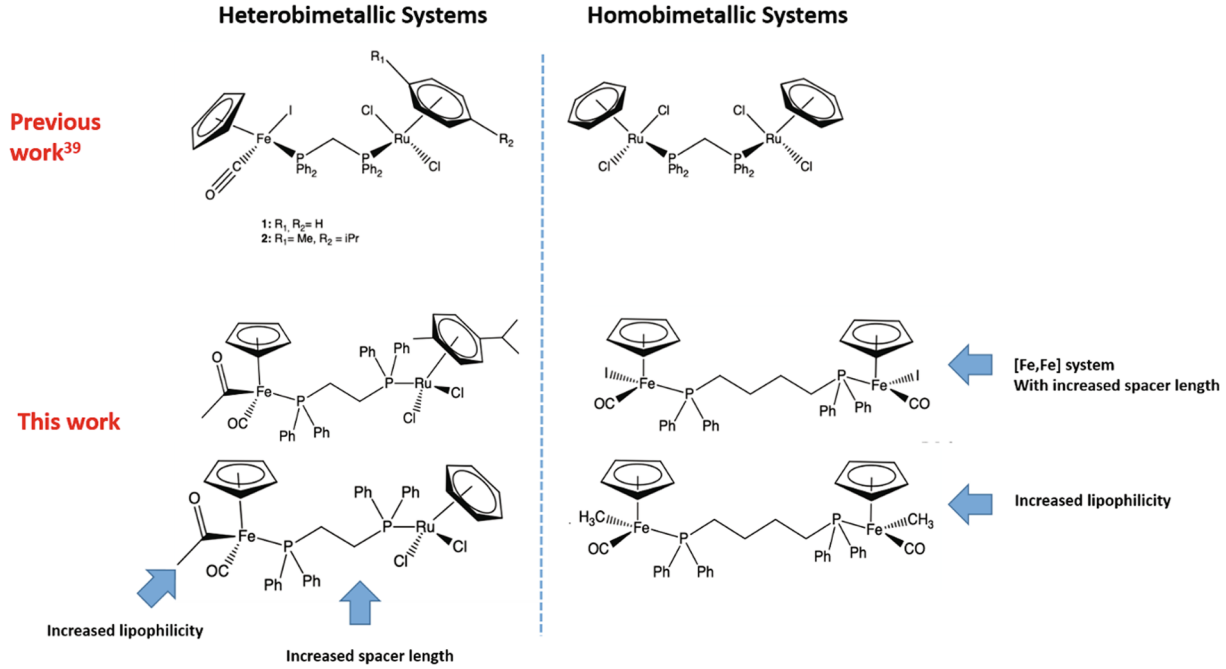

Fig. 1. Heterobimetallic and homobimetallic complexes reported which exhibit promising cytotoxic profiles and cancer cell selectivity and the compounds reported in the present study.

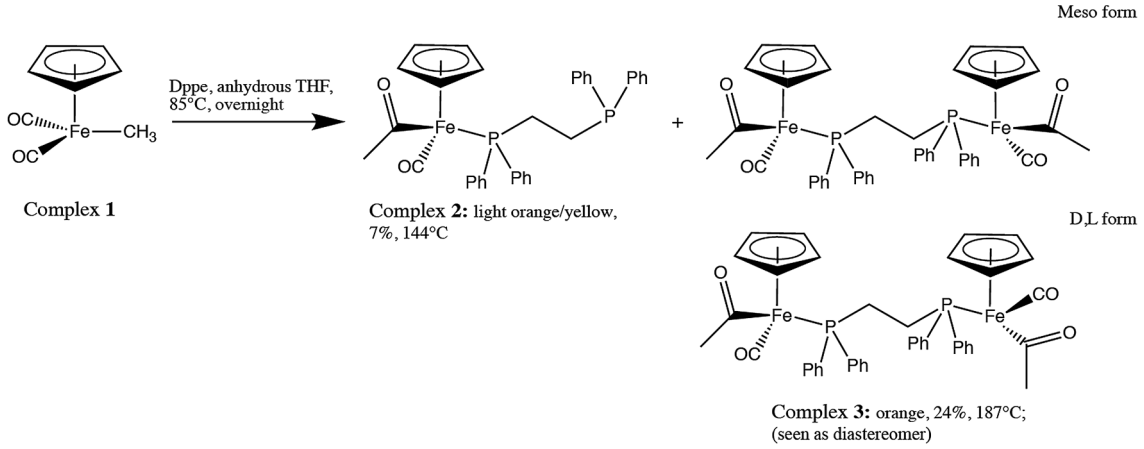

Scheme 1. Reaction scheme for the synthesis of products [CpFe(CO)($COCH_3$)(κ^1-dppe)] **2** and [[CpFe(CO)($COCH_3$)]$_2$(μ-dppe)] **3**. Complexes **2** and **3** possess asymmetric centres (Fe). For complex **2** this exists as a mixture of enantiomers (*rac*-**2**) (only one is depicted), while for complex **3** three stereoisomers are possible, i.e. the *meso* form and a set of enantiomers (only one is depicted in Scheme 1) [45].

The full spectroscopic characterization consisting of multinuclear NMR (^{1}H, ^{31}P{^{1}H}, ^{13}C{^{1}H}) FTIR, and ESI-MS, was carried out for both complexes. In complex **4**, a series of unresolved multiplet resonances in the range δ = 7.84 to 7.05 ppm correspond to the 20 aromatic protons in dppe. Four distinct doublets are observed from δ = 5.24 to 4.95 ppm, corresponding to the 4 inequivalent protons in the *p*-cymene ring, due to the asymmetry at the iron centre. The singlet resonance for η^5-C_5H_5 is observed at δ = 4.39 ppm, and the multiplet signals that follow from δ = 2.70 to 2.45 ppm correspond to the inequivalent protons in the dppe bridge. The consecutive singlets represent the methyl groups in the compound: the COCH_3 resonates at δ = 2.25 ppm and the CH_3 from the *p*-cymene is seen at δ = 1.84 ppm. Finally, the isopropyl methyl groups from the *p*-cymene substituent appear as 2 distinct doublet resonances at δ = 0.88 and 0.80 ppm respectively confirming the diastereotopic nature of the *i*Pr groups. The aromatic signals for complex **5** appear at similar ppm values to **4**. A singlet is observed at δ = 5.32 for complex **5**, and corresponds to 6 equivalent protons from the benzene (η^6-C$_6H_6$) substituent. Complex **5** shows the η^5-C_5H_5 resonance at δ = 4.39 ppm, as well as similar ppm values for the protons in the dppe bridge as with **4**. There is only one singlet resonance for the only methyl group in the compound (COCH_3), the latter which is seen at δ = 2.35 ppm. The ^{31}P{^{1}H} NMR spectra for complexes **4** and **5** are very similar and each contain two doublet resonances. A low-field shifted doublet signal for both complexes is seen at δ = 74.3 ppm, representing the Fe-*P*Ph$_2$ bond, while the second high-field shifted signal, also seen in both complexes, appears at δ = 25.1 ppm which corresponds to the Ru-*P*Ph$_2$ bond. The ^{13}C{^{1}H} NMR data for complex **4** shows a series of unresolvable multiplets from δ = 135.5 to 126.7 ppm for the carbon atoms in the aromatic substituents of dppe. Singlets which appear at δ = 107.4 and 93.4 ppm correspond to two C atoms on *p*-cymene ring, while the remaining carbon atoms within the *p*-cymene ring are represented by two sets doublets: one doublet appears at δ = 89.9 ppm due to ^{2}J(C,P) coupling. The singlets at δ = 83.6 ppm pertains to the equivalent carbons in the η^5-C_5H_5 group, and the doublet at δ = 50.9 ppm the methyl carbon from $COCH_3$ coupling to phosphorus atom.

Complex **5** shows similar ^{13}C{^{1}H} NMR features as **4**. The spectrum displays a doublet resonance at δ = 219.4 ppm with a ^{2}J(C,P) coupling constant of 30 Hz, for the Fe-*C*O. A singlet at δ = 87.6 ppm corresponds to the benzene substituent and the signal at δ = 83.7 ppm corresponds to η^5-*C*$_5$H$_5$. The FTIR spectra for complexes **4** and **5** reveal the strong stretching vibrations for both the Fe-(CO) and the Fe-(C=O)CH_3: For complex **4**, these are visible at ν = 1901 and 1581 cm^{-1} respectively, while for complex **5**, the stretching vibrations appear at 1897 and 1597 cm^{-1}. Both complexes were subjected to high resolution ESI-MS (+) and exhibit signals corresponding the radical cation [M]$^{\cdot+}$ and [M + Na]$^+$, both with matching isotope patterns confirming their constitution. In order to test the stability of the complexes in (DMSO, see

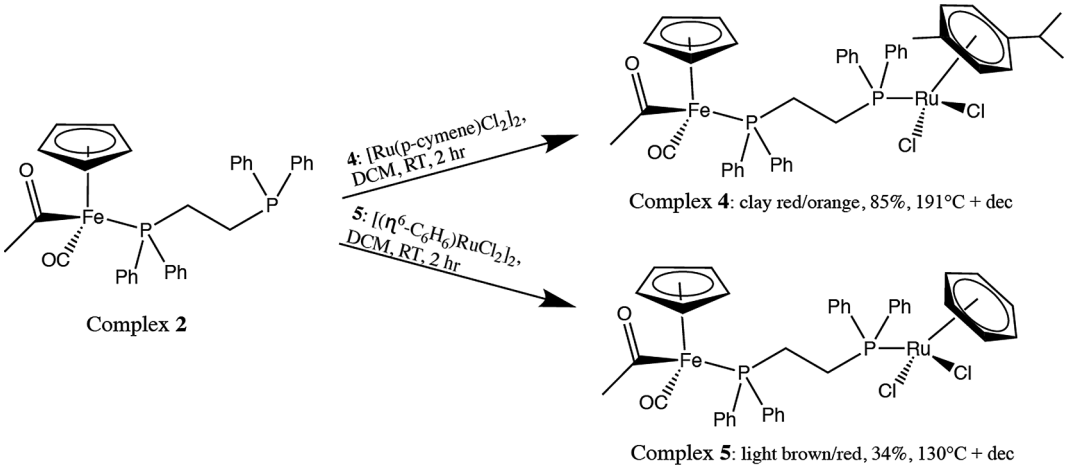

Scheme 2. Reaction scheme for the synthesis of complex [CpFe(CO)($COCH_3$)(μ-dppe)Ru(η^6-*p*-cymene)Cl$_2$] **4** and [CpFe(CO)($COCH_3$)(μ-dppe)Ru(η^6-C$_6H_6$)Cl$_2$] **5**. The iron centre in both complexes is asymmetric and complexes **4** and **5** exist as a racemic mixture (*rac*-**4** and *rac*-**5**). Only one stereoisomer is depicted for clarity in both cases.

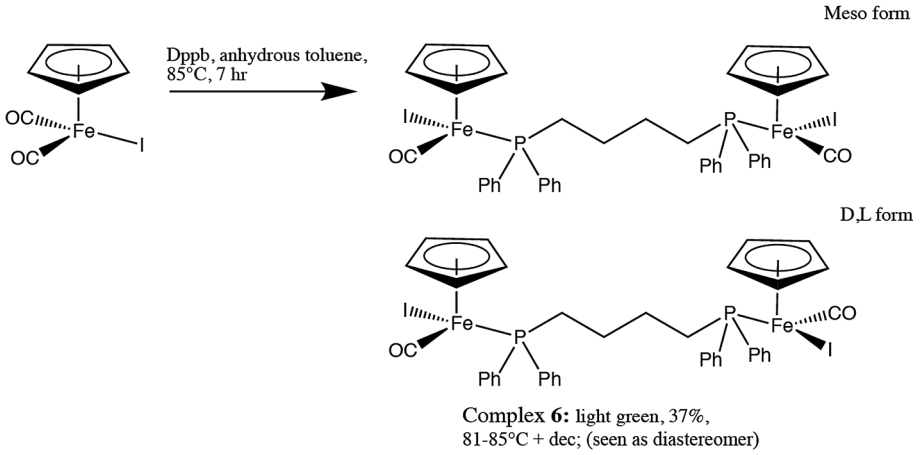

Scheme 3. Reaction scheme for the synthesis of complex **6** [[CpFe(CO)(I)]$_2$(μ-dppb)] · 0.5 hexane.

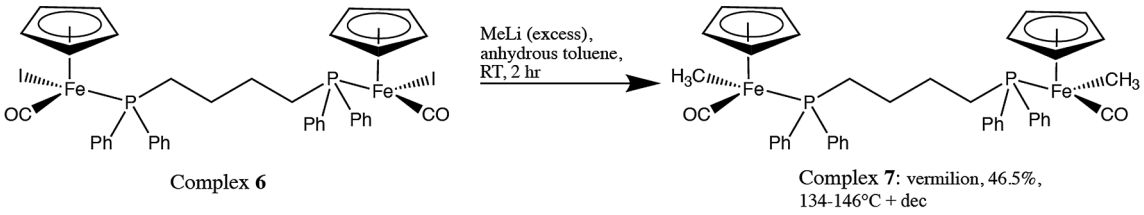

Scheme 4. Reaction scheme for the synthesis of complex **7** [[CpFe(CO)(CH$_3$)]$_2$(μ-dppb)] · 0.5 hexane.

below), $^{31}P\{^1H\}$ NMR spectra were recorded of complex **5** dissolved in DMSO-d_6 (containing water) after different time intervals [46]. The sample was tested each hour during the first 7 h, after 24 h, and finally after 72 h. When observing the spectra, it is evident that there are no changes in this time period.

We next targeted the homobimetallic [Fe,Fe] complex [[CpFe(CO)(I)]$_2$(μ-dppb)] (complex **6**), bearing the longer tether (dppb as opposed to dppe). We decided to use dppb to explore the effect of a longer spacer between the two metal centres, and to exclude formation of a κ^2-phosphine product. Surprisingly, homobimetallic complexes of the type [Fe(μ -phosphane)Fe], although highly prevalent in the literature and used *inter alia* as iron hydrogenase models, have altogether escaped investigation as potential anti-cancer agents, and herein we report the first such study (see below) [47]. The complex [CpFe(CO)$_2$I] and dppb (dppb = 1,1-bis(diphenylphosphino)butane)) was dissolved in toluene and refluxed at 85 °C for 7 h. The crude reaction mixture was purified by column chromatography using a 3:2 eluent mixture of dichloromethane/*n*-hexane which exhibited three separable bands. The third band corresponded to [[CpFe(CO)(I)]$_2$(μ-dppb)], which was isolated as a light green powder in a 37% yield (Scheme 3) as a mixture of stereoisomers.

Complex **6** exists as a mixture of three stereoisomers: a pair of enantiomers and a *meso* form akin to complex **3**. The complex was also subjected to full spectroscopic characterisation. The ^{1}H NMR spectrum reveals multiplet resonances from δ = 7.71 to 7.35 ppm correspond to the 20 protons of the phenyl rings of dppb, and a singlet at δ = 4.32 ppm with an integration of 10 protons corresponds to two equivalent η^5-C_5H_5 groups in the dinuclear compound. Two multiplet resonances at δ = 2.37 and 0.95 ppm respectively represent the protons of the dppb bridge. The remaining signals correspond to half a molecule of hexane included in the solid. In the $^{31}P\{^1H\}$ NMR spectrum, two singlets appear at δ = 61.7 ppm and δ = 61.6 ppm, akin to complex **3**; indicating the diasteriosomers in the *meso* form and pair of enantiomers in D,L form. The FTIR confirms the presence of one CO stretching vibration with a medium strong intensity at 1932 cm^{-1}. The ESI-MS spectra of **6** show a complex fragmentation pattern including the [M]$^+$ signal at 977.9068 m/z and a [M + Na]$^+$ signal at 1000.9033 m/z, which can be compare well to the theoretical values ([M]$^{\cdot+}$ 977.9129; for [M+Na]$^+$ 1000.9028) confirming constitution. $^{31}P\{^1H\}$ NMR spectra were also recorded of complex **6** in wet DMSO-d_6 after different time intervals, showing stability [46]. The compound, as with the [Fe,Ru] complexes shows stability over this time period (see SI for the spectra).

The related complex **7**, [[CpFe(CO)(CH$_3$)]$_2$(μ-dppb)] · 0.5 hexane, could readily be isolated upon reaction of complex **6** with MeLi (Scheme 4). After column chromatographic purification using CH_2Cl_2, the compound was successfully isolated as a vermilion powder with a yield of 46.5%. The complex is thermally robust and onset of colour change starts at 134 °C with full decomposition at 146 °C.

The ^{1}H NMR reveals the Fe-CH_3 resonance at δ = −0.29 ppm as a doublet of doublets due to coupling to P. In contrast to the precursor **6** the $^{31}P\{^1H\}$NMR spectrum shows only one singlet signal at δ = 75.5 ppm for the Fe-PPh$_2$ although two signals are expected due to the diasteriosomerism possibly due to isochronicity. In the FTIR

Table 1
IC_{50} (μM) values of complexes **2–7** on the A2780cisR cell-line after 72 h exposure to the compound. The values represent the mean between four replicates and ± the std. deviation.

Complex	IC_{50} (μM)
2	8.5 ± 0.1
3	>100
4	4.9 ± 0.4
5	6.5 ± 0.1
6	>100
7	61 ± 3
Cisplatin	35 ± 3
RAPTA-C	>200

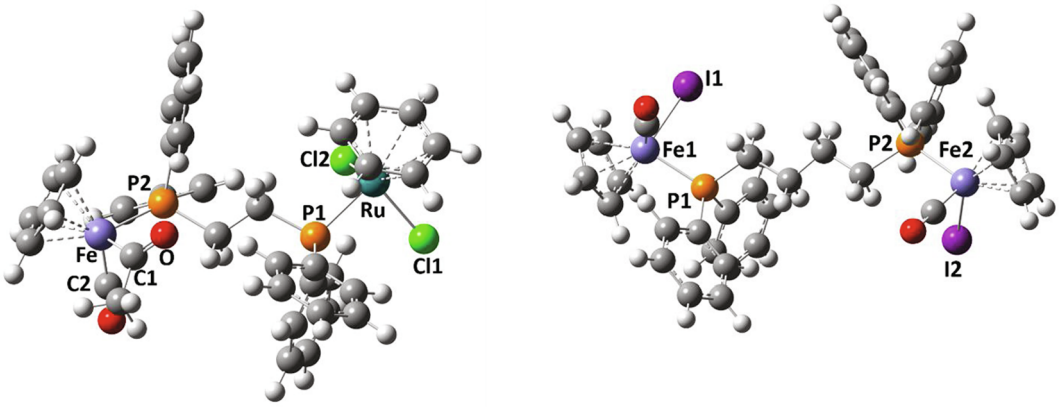

Fig. 2. DFT optimised structure of complex **5** (left). Selected bond lengths [Å]: Fe-P2 2.260, Ru-P1 2.387, Fe-C1 1.960, Fe-C2 1.749, Ru-Cl1 2.440, Ru-Cl2 2.466. Fe-P2-P1-Ru dihedral angle: 145°. DFT optimised structure of complex **6** (right). Selected bond lengths [Å] Fe1-I2/Fe2-I2 2.696, Fe1-P1/Fe2-P2 2.330, Fe1-$C_{carbonyl}$/Fe2-$C_{carbonyl}$ = 2.696. Fe1-P1-P2-Fe2 dihedral angle: 163°.

spectrum, the CO stretching vibration appears at ν = 1892 cm^{-1}, shifted by 40 wavenumbers from its precursor, **6**, due to enhanced electron density at the iron centre afforded by the methyl group.

Complexes **2–7** were subjected to *in vitro* cytotoxicity studies on the cisplatin resistant ovarian cancer cell line A2780cisR and compared to cisplatin as positive control and RAPTA-C as negative control (Table 1). In the series, the heterobimetallic [Fe,Ru] complexes **4** and **5** exhibit promising cytotoxic activity and are the most active in the series, with the cymene analogue **4** being slightly more cytotoxic than the benzene analogue **5**. This is in keeping with our earlier findings of related complexes bearing a dppm bridge between the Fe and Ru centres, i.e. [(η^6-C_6H_6)$RuCl_2$(μ-dppm)Fe(CO)I(η^5-C_5H_5)] (IC_{50} = 1.5 μM on A2780cisR) and [(η^6-*p*-cymene)$RuCl_2$(μ-dppm)Fe(CO)I(η^5-C_5H_5)] (IC_{50} = 1.2 μM or A2780cisR) [38a].

Interestingly, the bimetallic [Fe,Fe] complexes **3** and **6** are inactive with IC_{50} values > 100 μM, while the mononuclear iron complex **2** exhibits moderate activity. Complex **7**, the methylated analogue of **6**, exhibits some, albeit it low, cytotoxicity. These latter results suggest that increasing the lipophilicity of the ligand at the iron centre (I in **6** vs CH_3 in **7**) does enhance cytotoxicity, but overall the dinuclear [Fe,Fe] complexes are rather inactive.

Structural, electronic and spectroscopic characteristics for complexes **5** and **6** were calculated using density function theory methods (DFT). For all the calculations, the level of theory employed was B3LYP with the basis set 6-31 + G(d,p) for H, C, O, P and Cl atoms; while for I, Ru and Fe atoms DGDZVP basis set was used. Since we were unable to obtain suitable single crystals for X-ray diffraction analysis of the complexes, despite several attempts and crystallisation techniques, we obtained structural information of the complexes *via* DFT methods. Moreover, the calculated IR spectra of the optimised structures (in the gas phase), were compared to those obtained by experiment (solid state IR). These showed an excellent agreement, in both **5** and **6**, suggesting reasonable structural models for both complexes using DFT methods. Full identification and assignment of the vibrational modes in the IR spectra was also possible for **5** (see SI Fig. 5.5) and **6** (see SI Fig. 6.6) in light of this. Fig. 2 shows the optimised structures of complex **5** and **6** with some key metrical parameters obtained from DFT.

The most striking structural feature of both complexes is the zig-zag arrangement of the heavy atoms, with the two metal centres being somewhat *anti* with respect to each other. In complex **5** a Fe—P—P—Ru dihedral angle of 145° is observed, while complex **6** exhibited an Fe1-*P*1-*P*2-Fe2 dihedral angle of 163° (Fig. 3).

The electronic nature of complexes **5** and **6** was also studied. Fig. 4 shows the highest occupied molecular orbital (HOMO) and the lowest unoccupied molecular orbital (LUMO) with the corresponding molecular orbitals' energies of the two complexes.

Clear differences can readily be observed for the localizations of the HOMO and LUMO when comparing complexes **5** and **6**. For complex **5**, due to its asymmetrical nature, the HOMO and the LUMO are asymmetrically localized on the complex. In particular, the HOMO of complex **5** is delocalized on the iron metal and the ligands (Cp, CO, one phosphorous of the dppe and acetyl), while the LUMO is delocalized on the ruthenium terminus over the ligands (arene and chlorides) excluding the phosphorus atoms of the bridging dppe. This is in contrast to our earlier studies of related heterobimetallic [Fe,Ru] complexes, where *both* HOMO and LUMO were located on the iron terminus of the

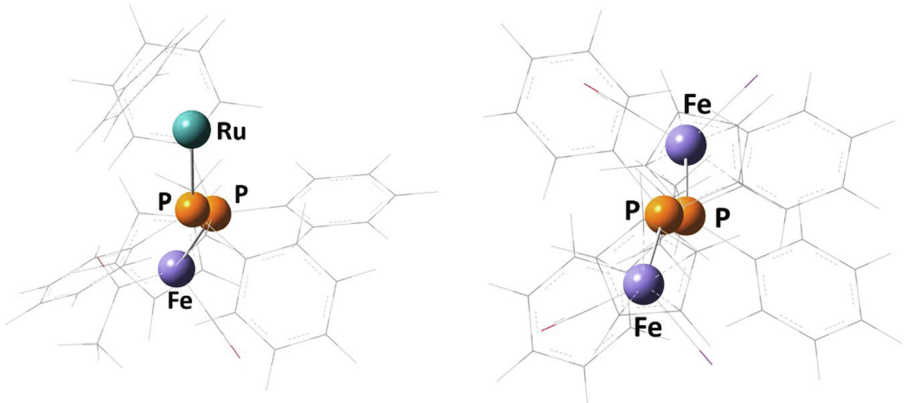

Fig. 3. Perspective of **5** (left) and **6** (right) viewed down the P—P vector. All atoms except the Fe,Ru and P are omitted for clarity.

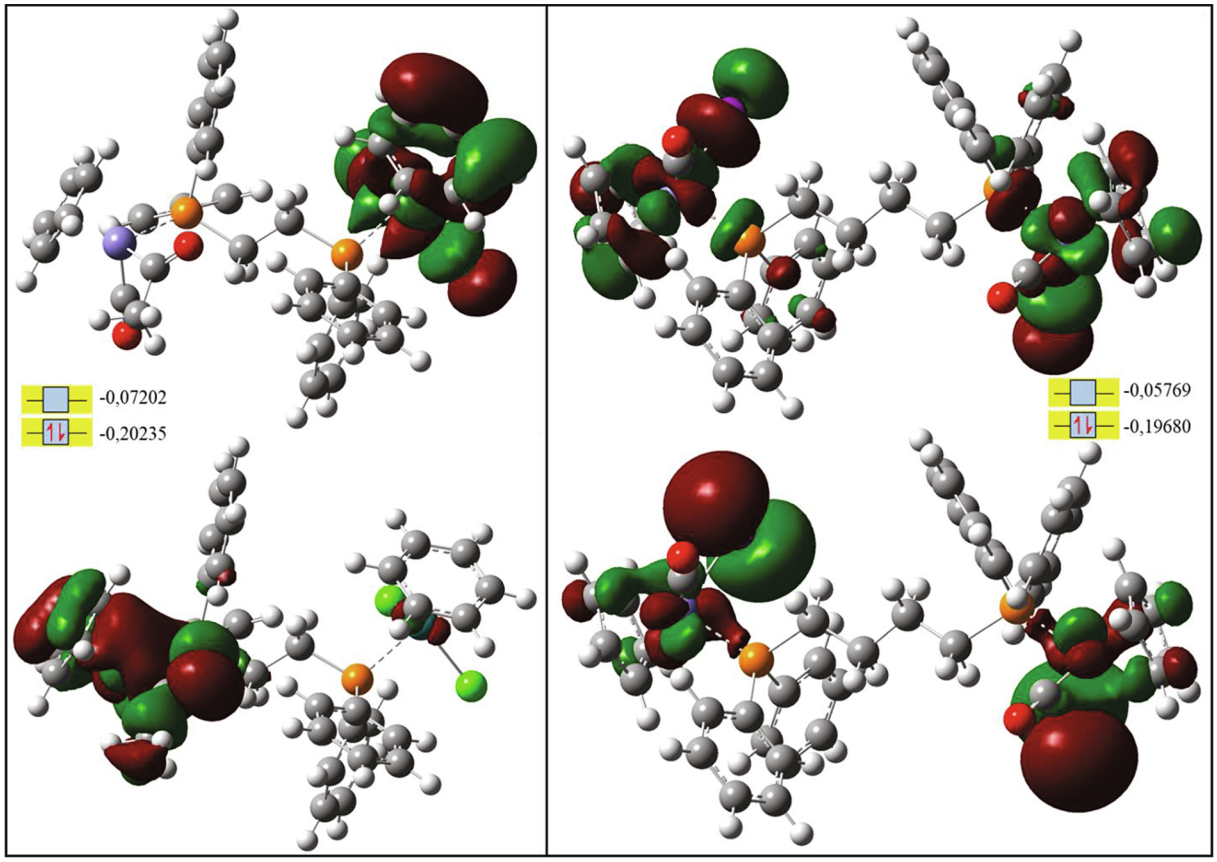

Fig. 4. LUMO (top) and HOMO (bottom) of the optimized structures of complex **5** (left) and **6** (right). The energies of the LUMOs (top) and HOMOs (bottom) are expressed in hartree. Blue = iron, red = oxygen, grey = carbon, orange = phosphorus, green = chlorine.

complex in [(η^6-Arene)$RuCl_2$(μ-dppm)Fe(CO)I(η^5-C_5H_5)] (Ar = C_6H_6 and *p*-cymene, dppm = 1,1-bis(diphenylphosphinomethane)) [38a]. The symmetric complex **6** shows the calculated HOMO and LUMO symmetrically localized on both metal centres with their corresponding ligands.

3. Conclusions

A series of heterobimetallic [Fe,Ru] and homobimetallic [Fe,Fe] complexes, bridged with a dppe ligand, were prepared and fully characterised spectroscopically and their structures, electronic nature and IR spectra investigated by DFT methods, the latter showing excellent agreement with experiment. The DFT study revealed that for the heterobimetallic complexes, the HOMO and LUMO are not both located on the iron terminus of the complex, in contrast to earlier findings [38a]. An *in vitro* study of all dinuclear complexes was carried out on the A2780cisR cisplatin resistant ovarian cancer cell-line, and compared to the known mononuclear iron complex [CpFe(CO)($COCH_3$)(κ^1-dppe)] **2**. While limited to only one-cell line, it can be seen that the heterobimetallic [Fe,Ru] complexes exhibit promising cytotoxicity profiles, while the corresponding [Fe,Fe] complexes exhibit very low activity; and the mononuclear complex **2** only moderate activity. Hence such homodinuclear [Fe,Fe] complexes, appear not be suitable candidates for further pursuit, whereas the [Fe,Ru] complexes have promising cytotoxicity [38a]. The increased spacer length, however, seems to slightly reduce cytotoxic action in the latter with the previously reported [Fe,Ru] complexes bearing a dppm bridge being somewhat more cytotoxic.

4. Experimental section

All reactions, unless stated otherwise, were performed under a nitrogen atmosphere using Schlenk procedures and/or glove-box manipulations. All solvents were degassed by bubbling nitrogen gas for several minutes through them and dried by passage over activated alumina. The starting materials were obtained from commercial suppliers and used as received. Dicarbonylcyclopentadienyliodoiron(II) ([CpFe$(CO)_2$I]) (97%), anhydrous tetrahydrofuran (99.9%), methyllithium (1.6 M in diethyl ether), dppe, dppb (99%) and silica gel (60 Å pore size, 70–230 mesh, 63–200 μm) were purchased from Sigma-Aldrich/Merck. Dichloromethane (stab. Amylene), as well as *n*-hexane and diethyl ether (stab. BHT), were obtained from Biosolve Chemicals. Ethyl acetate (99.5%) was purchased from VWR, as well as chloroform-*d* +0.03% TMS and dimethyl sulfoxide-d_6 (99.80%). Dry toluene (99.85%) was obtained from Acros Organics. Dichloro(*p*-cymene)ruthenium(II) dimer ([(*p*-cymene)$RuCl_2]_2$) (98%) was purchased from STREM, while benzeneruthenium(II)chloride dimer ([(benzene)$RuCl_2]_2$) (95%) was purchased from TCI. The known complexes **2** and **3** were prepared by modified literature procedures and can be found in the SI [42–44]. The apparatus used to measure the melting points was a Stuart SMP10 and are uncorrected. NMR experiments at room temperature were recorded using a Bruker Ultrashield 300 MHz/54 mm magnet system. Chemical shifts were observed relative to the residual solvent peak. The ^{1}H and ^{13}C {^{1}H} NMR chemical shifts were observed relative to tetramethylsilane (TMS), while for ^{31}P {^{1}H} NMR, they were measured relative to phosphoric acid (85%). The software for spectral analysis was Bruker Topspin 4.0.6. FTIR spectra were retrieved using a MIRacle 10 Shimadzu, with a single reflection ATR accessory. Per

sample, 64 scans were collected over a range of 400–4000 cm^{-1}, with a spectral resolution of 1 cm^{-1}; these were analysed using the IR solution software. UV–Vis spectra were obtained using a UV-188 spectrophotometer (Shimadzu) and quartz suprasil precision cells (100- QS, 10 mm light path, from Hellma Analytics). Finally, high resolution mass spectrometry (HR-ESI-MS) was recorded using a Bruker SolariX XR FT-ICR-MS in the Maastricht MultiModal Molecular Imaging Institute (M4I). The samples were dissolved in $CHCl_2$-CH_3CN- CH_3COOH (49.95 – 49.95 – 0.1%) and then diluted 100 times. The MS parameters were set in ionization + mode, with a capillary of 4.4 kV, end plate offset of −800 V, a nebulizer at 1 bar, dry gas at 4 L/min, a dry temperature of 200 °C, and a mass range of 300–1300 m/z. The resolution of all measurements was above 100000. Only the relevant signals are quoted in the experimental section. All isotope patterns were checked using online software; the isotope line with the highest intensity was reported for each sample.

5. Cytotoxicity tests

Human ovarian carcinoma (A2780cisR) cell lines were obtained from the European Collection of Cell CulturesPenicillin streptomycin, RPMI 1640 GlutaMAX (where RPMI = Roswell Park Memorial Institute), and DMEM GlutaMAX media (where DMEM = Dulbecco's modified Eagle medium) were obtained from Life Technologies, and fetal bovine serum (FBS) was obtained from Sigma. The cells were cultured in RPMI 1640 GlutaMAX (A2780cisR) and DMEM GlutaMAX (HEK-293) media containing 10% heat-inactivated FBS and 1% penicillin streptomycin at 37 °C and CO_2 (5%). The A2780cisR cell line was routinely treated with cisplatin (2 μM) in the media to maintain cisplatin resistance. The cytotoxicity was determined using the 3-(4,5-dimethyl 2-thiazolyl)-2,5-diphenyl-2H-tetrazolium bromide (MTT) assay [48]. Cells were seeded in flat-bottomed 96-well plates as a suspension in a prepared medium (100 μL aliquots and approximately 4300 cells/well) and pre-incubated for 24 h. Stock solutions of compounds were prepared in DMSO and were diluted in medium. The solutions were sequentially diluted to give a final DMSO concentration of 0.5% and a final compound concentration range (0–200 μM). Cisplatin and RAPTA-C were tested as a positive (0–100 μM) and negative (200 μM) controls respectively. The compounds were added to the preincubated 96-well plates in 100 μL aliquots, and the plates were incubated for a further 72 h. MTT (20 μL, 5 mg/mL in Dulbecco's phosphate buffered saline) was added to the cells, and the plates were incubated for a further 4 h. The culture medium was aspirated and the purple formazan crystals, formed by the mitochondrial dehydrogenase activity of vital cells, were dissolved in DMSO (100 μL/well). The absorbance of the resulting solutions, directly proportional to the number of surviving cells, was quantified at 590 nm using a SpectroMax M5e multimode microplate reader (using SoftMax Pro software, version 6.2.2). The percentage of surviving cells was calculated from the absorbance of wells corresponding to the untreated control cells. The reported IC_{50} values are based on 1 experiment comprising four tests per concentration level.

5.1. Density functional theory calculations

DFT calculations were performed to model the complexes **5** and **6**. Guassian09 software package was used. For all the calculations, the level of theory used for all calculations is B3LYP with the basis set 6-31 + G(d,p) for H, C, O, P and Cl atoms; while for I, Ru and Fe atoms DGDZVP basis set was used. Geometry optimizations were calculated without any constrains. All the optimized geometries show not imaginary frequency. Energies and infrared spectra were calculated on the optimized structures [49].

5.2. Synthesis of [CpFe(CO)($COCH_3$)(μ-dppe)Ru(η^6-p-cymene)Cl_2] (4)

0.048 g of [CpFe(CO)($COCH_3$)(μ^1-dppe)] (**2**) (0.081 mmol, 1 eq.) and 0.024 g of [(η^6-*p*-cymene)$RuCl_2$]$_2$ (0.040 mmol, 0.5 eq) were added to a 100 mL round bottom Schlenk flask. The reactants were dissolved in approximately 20 mL of dichloromethane; the solution was left to stir at room temperature for 2 h. The solvent was evaporated under reduced pressure, the residue washed with hexane, and the hexane washings discarded. The resulting solid was dried *in vacuo* affording a clay red/orange powder (0.0616 g, 0.068 mmol, 85%) with a decomposition temperature of 191 °C. ^{1}H NMR (300 MHz, $CDCl_3$, 298 K): δ 7.84–7.05 (20H, m, C-**H** dppe), 5.24 (1H, d, ^{3}J(H,H) = 6.20 Hz, *p*-cymene C-$\mathbf{H^D}$), 5.20 (1H, d, ^{3}J(H,H) = 6.20 Hz, *p*-cymene C-$\mathbf{H^C}$), 5.13 (1H, d, ^{3}J(H,H) = 6.20 Hz, *p*-cymene C-$\mathbf{H^B}$), 4.95 (1H, d, ^{3}J(H,H) = 6.20 Hz, *p*-cymene C-$\mathbf{H^A}$), 4.39 (5H, s, η^5-$C_5\mathbf{H_5}$), 2.70 (1H, m, C**H**Me_2), 2.49 (1H, m, PC$\mathbf{H^C}$ bridge), 2.47 (1H, m, PC$\mathbf{H^B}$ bridge), 2.45 (1H, m, PC$\mathbf{H^A}$ bridge), 2.25 (3H, s, CO$\mathbf{CH_3}$), 1.84 (3H, s, *p*-cymene C$\mathbf{H_3}$), 0.88 (3H, d, ^{3}J(H, H) = 7.02 Hz, *p*-cymene CH(C$\mathbf{H_3}$)$^{\mathbf{B}}$), 0.80 (3H, d, ^{3}J(H,H) = 7.02 Hz, *p*-cymene CH(C$\mathbf{H_3}$)$^{\mathbf{A}}$) ppm; ^{31}P{^{1}H} NMR ($CDCl_3$, 298 K): δ 74.3 (d, ^{3}J(P,P) = 34 Hz, Fe-**P**Ph_2), 25.1 (d, ^{3}J(P,P) = 34 Hz, Ru-**P**Ph_2) ppm; ^{13}C {^{1}H} NMR ($CDCl_3$, 298 K): δ 135.5–126.7 (m, dppe), 107.4 (s, *p*-cymene $\mathbf{C^{1\ or\ 4}}$-H), 93.4 (s, *p*-cymene $\mathbf{C^{1\ or\ 4}}$-H), 89.9 (d, ^{2}J(C,P) = 4.7 Hz, *p*-cymene $\mathbf{C^A}$-H), 88.6 (d, ^{2}J(C,P) = 3.8 Hz, *p*-cymene $\mathbf{C^B}$-H), 84.8 (d, ^{2}J(C,P) = 6.0 Hz, *p*-cymene $\mathbf{C^C}$-H), 84.1 (d, ^{2}J(C,P) = 5.7 Hz, *p*-cymene $\mathbf{C^C}$-H), 83.6 (s, η^5-$\mathbf{C_5}H_5$), 50.9 (d, ^{3}J(C,P) = 5.7 Hz, CO$\mathbf{C}H_3$), 28.9 (s, *p*-cymene $\mathbf{C}H(CH_3)_2$), 23.9 (m, dppe), 21.6 (s, *p*-cymene *i*Pr $\mathbf{C}H_3^{\mathbf{A}}$), 20.6 (s, *p*-cymene *i*Pr $\mathbf{C}H_3^{\mathbf{B}}$), 19.7 (d, ^{x}J(C,P) = 28.8 Hz, dppe),16.3 (s, *p*-cymene $\mathbf{C}H_3$) ppm; FTIR (cm^{-1}): ν = 3059 (vw), 1948 (w), 1901 (m, **CO** stretch), 1886 (m), 1581 (m, **CO** stretch), 1481 (w), 1435 (m), 1321 (w), 1261 (vw), 1178 (w), 1093 (w), 1060 (w), 999 (w), 906 (w), 889 (w), 819 (w), 748 (m), 717 (m), 694 (ms) cm^{-1}; ESI-MS: *m/z* Calcd. For $[M]^{\cdot+}$ 896.0745, found 896.0702. Calcd. For $[M + Na]^+$ 919.0635, found 919.0607.

5.3. Synthesis of [CpFe(CO)($COCH_3$)(μ-dppe)Ru(η^6-C_6H_6)Cl_2] (5)

0.100 g of [CpFe(CO)($COCH_3$)(μ^1-dppe)] (**2**) (0.169 mmol, 1 eq.) and 0.042 g of [(η^6-benzene)$RuCl_2$]$_2$ (0.084 mmol, 0.5 eq.) were added to a 100 mL Schlenk flask. The reactants were dissolved in approximately 20 mL of dichloromethane; the solution was left to stir at room temperature for 2 h. The solvent was evaporated under reduced pressure, and then column chromatography was performed in which a 1:1*n*-hexane/ethyl acetate eluent was utilized. The purification afforded a light brown/red powder (0.0477 g, 0.056 mmol, 34%) with a decomposition temperature of 130 °C. ^{1}H NMR (300 MHz, $CDCl_3$, 298 K): δ 7.73–7.14 (20H, m, C-**H** dppe), 5.32 (6H, s, η^6-$C_6\mathbf{H_6}$), 4.39 (5H, s, η^5-$C_5\mathbf{H_5}$), 2.70 (1H, m, PC$\mathbf{H^D}$ bridge), 2.46 (1H, m, PC$\mathbf{H^C}$ bridge), 2.40 (1H, m, PC$\mathbf{H^B}$ bridge), 2.35 (3H, s, CO$\mathbf{CH_3}$), 2.15 (1H, m, PC$\mathbf{H^A}$ bridge) ppm; ^{31}P{^{1}H} NMR ($CDCl_3$, 298 K): δ 74.3 (d, ^{3}J(P,P) = 38.5 Hz, Fe-**P**Ph_2), 25.1 (d, ^{3}J(P,P) = 38.5 Hz, Ru-**P**Ph_2) ppm; ^{13}C{^{1}H} NMR ($CDCl_3$, 298 K): δ 219.4 (d, ^{2}J(C,P) = 30 Hz, Fe-**C**O), 135.6–127.0 (m, dppe), 87.6 (d, ^{2}J(C,P) = 3.5 Hz, η^6-$\mathbf{C_6}H_6$) 83.7 (s, η^5-$\mathbf{C_5}H_5$), 50.7 (d, ^{3}J(C,P) = 5 Hz, CO$\mathbf{C}H_3$), 24.9 (d, ^{1}J(C,P) = 27 Hz, $\mathbf{C^B}H_2PPh_2$ bridge), 21.1 (d, ^{1}J(C,P) = 27 Hz, $\mathbf{C^A}H_2PPh_2$ bridge) ppm; FTIR: ν = 3072 (vw), 2962 (vw), 2897 (vw), 2474 (vw), 2312 (vw), 1897 (ms, **CO** stretch), 1734 (vw), 1597 (m, **CO** stretch) 1500 (vw), 1481 (w), 1433 (mw), 1411 (w), 1373 (vw), 1319 (vw), 1259 (w), 1176 (w), 1095 (s), 1055 (s), 1028 (ms), 1014 (ms), 898 (w), 887 (w), 842 (w), 821 (ms), 800 (ms), 746 (ms), 725 (ms), 717 (s), 692 (s), 621 (w), 611 (w), 584 (w), 574 (w), 561 (w), 414 (w) cm^{-1} (Full assignment of all stretching vibrations can be found in SI, secured by DFT); ESI-MS: *m/z* Calcd. For $[M]^{\cdot+}$ 840.0117, found 840.0085. Calcd. For $[M + Na]^+$ 863.0015, found 862.9983.

5.4. Synthesis of [[CpFe(CO)(I)]$_2$(μ-dppb)] · 0.5 hexane (6)

0.100 g of [CpFe(CO)$_2$I] (0.329 mmol) and 0.121 g of 1,4-Bis(diphenylphosphino)butane (dppb) (0.284 mmol) were added to a 100 mL round bottom Schlenk flask. The reactants were dissolved in 30 mL of

dry toluene. The reaction was left to stir under a reflux at 85 °C for 7 h. The solution was then cooled to room temperature and filtered under gravity. The remaining mixture was dried in *vacuo* and was purified using column chromatography with an eluent consisting of 3:2 dichloromethane/*n*-hexane. The first band was a light brown colour, which was discarded. The second band was light green, which was contaminated with starting dppb. The desired product, [[CpFe(CO)(I)]$_2$(μ-dppb)], was concentrated in the third dark green band. The latter was dried *in vacuo,* which afforded a light green powder with a yield of 0.101 g (0.103 mmol, 37%) and a decomposition temperature of 81–85 °C. ^{1}H NMR (300 MHz, $CDCl_3$, 298 K): δ 7.71–7.35 (20H, m, C-**H** dppb), 4.32 (10*H*, s, η^5-C$_5$**H$_5$**), 2.37 (4H, m, PC**H^A** bridge), 1.25 (5H, br s, C**H$_2$** hexane), 0.95 (4H, m, PC**H^B** bridge), 0.87 (1H, m, C**H$_3$** hexane) ppm (assigned by HSQC/HMBC experiments); ^{31}P{^{1}H} NMR ($CDCl_3$, 298 K): δ 61.7 (s, Fe-**P**Ph$_2$, *meso* stereoisomer and/or D,L form), 61.6 (s, Fe-**P**Ph$_2$, *meso* stereoisomer and/or D,L form) ppm; ^{13}C{^{1}H} NMR ($CDCl_3$, 298 K): δ 220.7 (s, Fe-**C**O), 133.1–131.7(m, **C**−H dppb), 130.4 (s, **C** quaternary dppb), 128.6–128.2 (m, **C**−H dppb), 82.4 (s, η^5-**C$_5$**H$_5$), 33.3 (d, ^{1}J(C,P) = 17.5 Hz, **C^A**H$_2$PPh$_2$ bridge), 32.9 (d, ^{1}J(C,P) = 17.5 Hz, **C^B**H$_2$PPh$_2$ bridge), 31.6 (s, **C**H$_2$(3) hexane), 25.2 (s, **C^A**H$_2$ bridge), 25.1 (s, **C^B**H$_2$ bridge), 22.7 (s, **C**H$_2$(2) hexane), 14.1 (s, **C**H$_3$ hexane) ppm; FTIR (cm^{-1}): ν = 2953 (w), 2924 (w), 2854 (w), 1932 (ms, **CO** stretch), 1587 (vw), 1571 (vw), 1479 (w), 1433 (w), 1359 (vw), 1307 (vw), 1259 (vw), 1180 (w), 1157 (w), 1093 (w), 1070 (w), 1026 (w), 999 (w), 839 (w), 821 (w), 740 (m), 719 (w), 694 (s), 617 (vw), 596 (w), 569 (w), 553 (w), 536 (w), 447 (vw), 418 (vw), 412 (vw) cm^{-11} (Full assignment of all stretching vibrations can be found in SI, secured by DFT); UV–Vis (nm)/ dichloromethane λ$_{max}$: λ 615 (minor), 436 (major); ESI-MS: *m/z* Calcd. For [M]$^{\cdot+}$ 977.9135, found 977.9068. Calcd. For [M + Na]$^+$ 1000.9033, found 1000.8967.

5.5. Synthesis of [[CpFe(CO)(CH$_3$)]$_2$(μ-dppb)] · 0.5 hexane (7)

0.243 g of [[CpFe(CO)(I)]$_2$(μ-dppb)] (0.248 mmol) were added to a 100 mL round bottom flask, containing 50 mL of degassed toluene. The dark green solution was cooled to approximately −80 °C, and MeLi (0.341 mL, 0.546 mmol, 2.2 eq) was carefully added in a dropwise fashion, turning the solution brown. The mixture was removed from the cooling bath and allowed to warm to ambient temperature, and then was left to stir for 2 h, which darkened the colour of the brown solution. The solvent was evaporated under reduced pressure. The air-stable dark brown solid was purified *via* column chromatography using CH_2Cl_2 as the eluent, and then washed with hexane. The latter yielded 0.087 g of a vermilion-coloured powder (0.115 mmol, 46.5%) with a decomposition temperature of 134–146 °C. ^{1}H NMR (300 MHz, $CDCl_3$, 298 K): δ 7.62–7.29 (20H, m, C-**H** dppb), 4.12 (10*H*, s, η^5-C$_5$**H$_5$**), 1.94 (4H, m, bridge), 1.25 (4H, s, C**H$_2$** hexane), 1.16 (2H, m, bridge), 0.92 (2H, m, bridge), 0.88 (1H, m, C**H$_3$** hexane), −0.29 (6H, dd, ^{3}J(H,P) = 8.0 Hz & 6.40 Hz, C**H$_3$**) ppm; ^{31}P {^{1}H} NMR ($CDCl_3$, 298 K): δ 75.5 (s, Fe-**P**Ph$_2$) ppm; FTIR (cm^{-1}): ν = 3059 (vw), 2924 (w), 2870 (w), 1892 (s, **CO** stretch), 1718 (vw), 1684 (vw), 1653 (vw), 1647 (vw), 1586 (vw), 1571 (vw), 1479 (w), 1458 (w), 1432 (m), 1360 (vw), 1329 (vw), 1306 (w), 1291 (vw), 1260 (w), 1181 (w), 1170 (w), 1157 (w), 1093 (m), 1070 (m), 1058 (m), 1027 (m), 1011 (m), 999 (m), 891 (vw), 840 (m), 818 (m), 801 (m), 743 (m), 738 (m), 723 (m), 693 (vs), 618 (vw), 603 (w), 593 (w), 576 (w), 545 (vw), 535 (vw), 462 (vw) cm^{-1}. ESI-MS: *m/z* Calcd. For [M]$^{\cdot+}$ 754.1515, found 754.1524 (17%). Calcd. For [M-CpFe(CO)(CH$_3$)]$^+$ 590.1591, found 590.1558 (100%).

Declaration of Competing Interest

The authors declare that they have no known competing financial interests or personal relationships that could have appeared to influence the work reported in this paper.

Acknowledgement

We thank the Maastricht Science Programme (MSP) and Maastricht University (Faculty of Science and Engineering) for financial support of this research. We also thank Maarten Honing, Peilang Han and Darya Hadavi (M4I, FHML (Maastricht MultiModal Molecular Imaging; Faculty Health, Medicine & Life Sciences, Maastricht University) for measuring the HRMS of all the compounds. Dr. Christian Bahn (MSP) is also thanked for useful discussions on the stereochemistry of the complexes.

Associated Content.

The supporting information is available free of charge. Supporting Information is available containing the synthesis and characterisation of known complexes, Multinuclear NMR, IR (experimental and calculated) and ESI-MS spectra of the compounds reported here and Cartesian coordinates for the complexes studied by DFT methods.

Appendix A. Supplementary data

Supplementary data to this article can be found online at https://doi.org/10.1016/j.ica.2020.119731.

References

[1] (a) WHO, Cancer, Geneva: World Health Organization, September 2018, https://www.who.int/news-room/fact-sheets/detail/cancer (accessed Sep 18, 2019).
(b) V. Tamizhazhagan, K. Pugazhendy, V. Sakthidasan, C. Jayanthi, S. Rajesh, P. Manikanadan, Social and economic burden of cancer on 2020-minireview, Cancer Res. J. 6 (2018) 10–15;
(c) R.L. Siegel, K.D. Miller, A. Jemal, Cancer statistics, 2020, CA: Cancer J. Clinic. 70 (2020) 7–30

[2] V.T. DeVita, E. Chu, A history of cancer chemotherapy, Cancer Res. 68 (2008) 8643–8653.

[3] A. Caley, R. Jones, The principles of cancer treatment by chemotherapy, Surgery (Oxford) 30 (2012) 186–190.

[4] (a) See as examples: S. Rafique, M. Idrees, A. Nasim, H. Akbar, A. Athar, Transition metal complexes as potential therapeutic agents, Biotechnol. Mol. Biol. Rev. 5 (2010) 38–45;
(b) P.V. Simpson, N.M. Desai, I. Casari, M. Massi, M. Falasca, Metal-based antitumor compounds: beyond cisplatin, Future Medicinal Chemistry 11 (2019) 119–135;
(c) M. Zaki, S. Hairat, E.S. Aazam, Scope of organometallic compounds based on transition metal-arene systems as anticancer agents: starting from the classical paradigm to targeting multiple strategies, RSC Adv. 9 (2019) 3239–3278;
(d) U. Ndagi, N. Mhlongo, M.E. Soliman, Metal complexes in cancer therapy – an update from drug design perspective, Drug Design Develop. Therapy 11 (2017) 599–616;
(e) W. Liu, R. Gust, Update on metal N-heterocyclic carbene complexes as potential anti-tumor metallodrugs, Coord. Chem. Rev. 329 (2016) 191–213.

[5] (a) See as examples: B. Rosenberg, Cisplatin: Its History and Possible Mechanisms of Action, Elsevier, Cisplatin, 1980, pp. 9–20;
(b) F.M. Muggia, A. Bonetti, J.D. Hoeschele, M. Rozencweig, S.B. Howell, Platinum antitumor complexes: 50 years since Barnett Rosenberg's discovery, J. Clin. Oncol. 33 (2015) 4219–4226.

[6] (a) See as examples: D. Chen, V. Milacic, M. Frezza, Q.P. Dou, Metal complexes, their cellular targets and potential for cancer therapy, Curr. Pharm. Des. 15 (2009) 777–791;
(b) M.S. Hassan, A.M. Morgan, M.M. Mekawy, M.A. Zeineb, Molecular mechanisms of Cisplatin-induced placental toxicity and teratogenicity in rats and the ameliorating role of N-acetyl-cysteine, Int. J. Biochem. Cell-Biol. 115 (2019);
(c) M. Raudenska, J. Balvan, M. Fojtu, J. Gumulec, M. Masarik, Unexpected therapeutic effects of cisplatin, Metallomics 11 (2019) 1182–1199;
(d) W. Zeng, Z. Du, Q. Luo, Y. Zhao, Y. Wang, K. Wu, F. Jia, Y. Zhang, F. Wang, Proteomic strategy for identification of proteins responding to cisplatin-damaged DNA, Anal. Chem. 91 (2019) 6035–6042;
(e) D. Sheikh-Hamad, Cisplatin-induced cytotoxicity: is the nucleus relevant? Am. J. Physiol. Renal Physiol. 295 (2008) F42–F43;
(f) D.B. Zamble, S.J. Lippard, Cisplatin and DNA repair in cancer chemotherapy, Trends Biochem. Sci. 20 (1995) 435–439;
(g) J. Kozelka, J.C. Chottard, How does cisplatin alter DNA structure? a molecular mechanics study on double-stranded oligonucleotides, Biophys. Chem. 35 (1990) 165-1.

[7] M.S. Davies, S.J. Berners-Price, T.W. Hambley, Slowing of cisplatin aquation in the presence of DNA but not in the presence of phosphate: improved understanding of sequence selectivity and the roles of monoaquated and diaquated species in the binding of cisplatin to DNA, Inorg. Chem. 39 (2000) 5603–5613.

[8] R.A. Alderden, M.D. Hall, T.W. Hambley, The discovery and development of cisplatin, J. Chem. Educ. 83 (2006) 728.

[9] E. Wong, C.M. Giandomenico, Current status of platinum-based antitumor drugs, Chem. Rev. 99 (1999) 2451–2466.

[10] B. Lippert, Cisplatin: Chemistry and Biochemistry of a Leading Anticancer Drug,

John Wiley & Sons, 1999.
[11] S. Dasari, P.B. Tchounwou, Cisplatin in cancer therapy: molecular mechanisms of action, Eur. J. Pharmacol. 740 (2014) 364–378.
[12] T.W. Hambley, The influence of structure on the activity and toxicity of Pt anticancer drugs, Coord. Chem. Rev. 166 (1997) 181–223.
[13] N.J. Wheate, S. Walker, G.E. Craig, R. Oun, The status of platinum anticancer drugs in the clinic and in clinical trials, Dalton Trans. 39 (2010) 8113–8127.
[14] R.S. Go, A.A. Adjei, Review of the comparative pharmacology and clinical activity of cisplatin and carboplatin, J. Clin. Oncol. 17 (1999) 409–409.
[15] A. Ahmad, F. Sarkar, Breast Cancer Metastasis and Drug Resistance, Progress and Prospects, Springer, 2013.
[16] (a) See: I. Ott, R. Gust, Non platinum metal complexes as anti-cancer drugs, Archiv Pharmazie Int. J. Pharmac. Med. Chem. 340 (2007) 117–126;
(b) And further examples: E.Y. Tshuva, M. Miller, Coordination complexes of titanium(IV) for anticancer therapy, Metal Ions Life Sci. 18 (2018) 219–250;
(c) H. Skoupilova, R. Hrstka, M. Bartosik, Titanocenes as anticancer agents: recent insights, Med. Chem. (Sharjah, United Arab Emirates) 13 (2017) 334–344;
(d) P. Beckhove, O. Oberschmidt, A.R. Hanauske, C. Pampillon, V. Schirrmacher, N.J. Sweeney, K. Strohfeldt, M. Tacke, Antitumor activity of Titanocene Y against freshly explanted human breast tumor cells and in xenografted MCF-7 tumors in mice, Anticancer Drugs 18 (2007) 311–315;
(e) O. Oberschmidt, A.-R. Hanauske, F.-J.K. Rehmann, K. Strohfeldt, N. Sweeney, M. Tacke, Activity of [1,2-di(cyclopentadienyl)-1,2-di(p-N, N-dimethylaminophenyl)-ethanediyl] titanium dichloride against tumor colony-forming units, Anticancer Drugs 16 (2005) 1071–1073.
[17] (a) See as selected examples: G. Marcon, S. Carotti, M. Coronnello, L. Messori, E. Mini, P. Orioli, T. Mazzei, M.A. Cinellu, G. Minghetti, Gold (III) complexes with bipyridyl ligands: solution chemistry, cytotoxicity, and DNA binding properties, J. Med. Chem. 45 (2002) 1672–1677;
(b) J.H. Sze, P.V. Raninga, K. Nakamura, M. Casey, K.K. Khanna, S.J. Berners-Price, G. Di Trapani, K.F. Tonissen, Anticancer activity of a Gold(I) phosphine thioredoxin reductase inhibitor in multiple myeloma, Redox Biol. 28 (2020);
(c) J.H. Kim, E. Reeder, S. Parkin, S.G. Awuah, Gold(I/III)-phosphine complexes as potent antiproliferative agents, Sci. Rep. 9 (2019) 1–18;
(d) N. Estrada-Ortiz, E. Lopez-Gonzales, B. Woods, S. Stuerup, I.A.M. de Graaf, G.M.M. Groothuis, A. Casini, Ex vivo toxicological evaluation of experimental anticancer gold(I) complexes with lansoprazole-type ligands, Toxicol. Res. (Cambridge, UK) 8 (2019) 885–895;
(e) F. Guarra, T. Marzo, M. Ferraroni, F. Papi, C. Bazzicalupi, P. Gratteri, G. Pescitelli, L. Messori, T. Biver, C. Gabbiani, Interaction of a gold(I) dicarbene anticancer drug with human telomeric DNA G-quadruplex: solution and computationally aided X-ray diffraction analysis, Dalton Trans. 47 (2018) 16132–16138;
(f) C.I. Yeo, K.K. Ooi, E.R.T. Tiekink, Gold-based medicine: a paradigm shift in anticancer therapy, Molecules 23 (2018) 1410–1426;
(g) I. Marmol, P. Castellnou, R. Alvarez, M.C. Gimeno, M.J. Rodriguez-Yoldi, E. Cerrada, Alkynyl Gold(I) complexes derived from 3-hydroxyflavones as multitargeted drugs against colon cancer, Eur. J. Med. Chem. 183 (2019).
[18] A.R. Simović, R. Masnikosa, I. Bratsos, E. Alessio, Chemistry and reactivity of ruthenium (II) complexes: DNA/protein binding mode and anticancer activity are related to the complex structure, Coord. Chem. Rev. 398 (2019) 113011.
[19] P. Schluga, C.G. Hartinger, A. Egger, E. Reisner, M. Galanski, M.A. Jakupec, B.K. Keppler, Redox behavior of tumor-inhibiting ruthenium (III) complexes and effects of physiological reductants on their binding to GMP, Dalton Trans. (2006) 1796–1802.
[20] E.S. Antonarakis, A. Emadi, Ruthenium-based chemotherapeutics: are they ready for prime time? Cancer Chemother. Pharmacol. 66 (2010) 1–9.
[21] E. Musgrove, C. Rugg, I. Taylor, D. Hedley, Transferrin receptor expression during exponential and plateau phase growth of human tumour cells in culture, J. Cell. Physiol. 118 (1984) 6–12.
[22] H. Yamada, T. Koike, J.K. Hurst, Water exchange rates in the diruthenium μ-Oxo Ion cis, cis-$[(bpy)_2Ru(OH_2)]_2O^{4+}$, J. Am. Chem. Soc. 123 (2001) 12775–12780.
[23] G. Sava, S. Pacor, A. Bergamo, M. Cocchietto, G. Mestroni, E. Alessio, Effects of ruthenium complexes on experimental tumors: irrelevance of cytotoxicity for metastasis inhibition, Chem. Biol. Interact. 95 (1995) 109–126.
[24] J.M. Rademaker-Lakhai, D. van den Bongard, D. Pluim, J.H. Beijnen, J.H. Schellens, A phase I and pharmacological study with imidazolium-trans-DMSO-imidazole-tetrachlororuthenate, a novel ruthenium anticancer agent, Clin. Cancer Res. 10 (2004) 3717–3727.
[25] A. Bergamo, R. Gagliardi, V. Scarcia, A. Furlani, E. Alessio, G. Mestroni, G. Sava, In vitro cell cycle arrest, in vivo action on solid metastasizing tumors, and host toxicity of the antimetastatic drug NAMI-A and cisplatin, J. Pharmacol. Exp. Ther. 289 (1999) 559–564.
[26] A. Bergamo, C. Gaiddon, J. Schellens, J. Beijnen, G. Sava, Approaching tumour therapy beyond platinum drugs: status of the art and perspectives of ruthenium drug candidates, J. Inorg. Biochem. 106 (2012) 90–99.
[27] A.F. Peacock, P.J. Sadler, Medicinal organometallic chemistry: designing metal arene complexes as anticancer agents, Chem.–Asian J. 3 (2008) 1890–1899.
[28] B.S. Murray, M.V. Babak, C.G. Hartinger, P.J. Dyson, The development of RAPTA compounds for the treatment of tumors, Coord. Chem. Rev. 306 (2016) 86–114.
[29] S. Inoue, S. Kawanishi, Hydroxyl radical production and human DNA damage induced by ferric nitrilotriacetate and hydrogen peroxide, Cancer Res. 47 (1987) 6522–6527.
[30] S.V. Torti, F.M. Torti, Iron and cancer: more ore to be mined, Nat. Rev. Cancer 13 (2013) 342.
[31] E. Hillard, A. Vessières, L. Thouin, G. Jaouen, C. Amatore, Ferrocene-mediated proton-coupled electron transfer in a series of ferrocifen-type breast-cancer drug candidates, Angew. Chem. Int. Ed. 45 (2006) 285–290.
[32] D. Serra, K.A. Abboud, C.R. Hilliard, L. McElwee-White, Electronic interactions in iron-and ruthenium-containing heterobimetallic complexes: structural and spectroscopic investigations, Organometallics 26 (2007) 3085–3093.
[33] M. Wenzel, E. Bigaeva, P. Richard, P. Le Gendre, M. Picquet, A. Casini, E. Bodio, New heteronuclear gold (I)–platinum (II) complexes with cytotoxic properties: are two metals better than one? J. Inorg. Biochem. 141 (2014) 10–16.
[34] J. Fernández-Gallardo, B.T. Elie, M. Sanaú, M. Contel, Versatile synthesis of cationic N-heterocyclic carbene–gold (I) complexes containing a second ancillary ligand. Design of heterobimetallic ruthenium–gold anticancer agents, Chem. Commun. 52 (2016) 3155–3158.
[35] O. Renier, C. Deacon-Price, J. Peters, K. Nurekeyeva, C. Russon, S. Dyson, S. Ngubane, J. Baumgartner, P. Dyson, T. Riedel, Synthesis and In vitro (anticancer) evaluation of η^6-arene ruthenium complexes bearing stannyl ligands, Inorganics 5 (2017) 44.
[36] M. Gras, B. Therrien, G. Süss-Fink, A. Casini, F. Edafe, P.J. Dyson, Anticancer activity of new organo-ruthenium, rhodium and iridium complexes containing the 2-(pyridine-2-yl)thiazole N N-chelating ligand, J. Organomet. Chem. 695 (2010) 1119–1125.
[37] C. Deacon-Price, D. Romano, T. Riedel, P.J. Dyson, B. Blom, Synthesis, characterisation and cytotoxicity studies of ruthenium arene complexes bearing trichlorogermyl ligands, Inorg. Chim. Acta 484 (2019) 513–520.
[38] (a) B. Herry, L.K. Batchelor, B. Roufosse, D. Romano, J. Baumgartner, M. Borzova, T. Reifenstahl, T. Collins, A. Benamrane, J. Weggelaar, M.C. Correia, P.J. Dyson, B. Blom, Heterobimetallic Ru(μ-dppm)Fe and homobimetallic Ru(μ-dppm)Ru complexes as potential anti-cancer agents, J. Organom. Chem. (2019);
(b) For μ-dppm (or similar) bridged Fe,Ru complexes see: N. Nawar, A.K. Smith, Syntheses of ruthenium-containing heterometallic complexes by use of tridentate phosphine ligands, J. Organom. Chem. 493 (1995) 239–242;
(c) A.W. Coleman, D.F. Jones, P.H. Dixneuf, C. Brisson, J.J. Bonnet, G. Lavigne, Dehalogenation of binuclear arene-ruthenium complexes: a new route to homonuclear triruthenium and heteronuclear ruthenium-iron cluster complexes containing chelating phosphorus ligands. Crystal structure of $Ru_3(CO)_{10}(Ph_2PCH_2PPh_2)$, Inorganic Chem. 23 (1984) 952–956;
(d) P.A. Dolby, M.M. Harding, N. Newar, A.K. Smith, Syntheses of iron-containing heterometallic complexes using tridentate phosphine ligands; the crystal structure of $[(OC)_3Fe\{(Ph_2P)_2CHCH_2PPh_2]Ru_3(CO)_9\{Ph_2PC(CH_2)PPh_2\}]$, J. Chem. Soc., Dalton Trans (1992) 2939–2942;
(e) M.-G. Mendoza-Ferri, C.G. Hartinger, R.E. Eichinger, N. Stolyarova, K. Severin, M.A. Jakupec, A.A. Nazarov, B.K. Keppler, Influence of the spacer length on the in vitro anticancer activity of dinuclear ruthenium-arene compounds, Organometallics 27 (2008) 2405–2407.
[39] (a) R.A. Zelonka, M.C. Baird, Canad. J. Chem. 50 (18) (1972) 3063–3072;
(b) M.A. Bennett, A.K. Smith, J. Chem. Soc. Dalton Trans. (1974) 233–241.
[40] J.K. Pagano, B.J. Ackley, R. Waterman, Evidence for iron-catalyzed α-phosphinidene elimination with phenylphosphine, Chem. Eur. J. 24 (2018) 2554–2557.
[41] For spectra shifts see: A. Munyaneza, O.G. Adeyemi, N.J. Coville, Solventless migratory-insertion reactions of substituted cyclopentadienyl iron complexes induced by electron donor ligands, Bull. Chem. Soc. Ethiop. 23 (3) (2009) 399–407.
[42] L.-S. Luh, L.-K. Liu, Synthesis and X-ray Structure of $[(\eta^5\text{-}C_5H_5)Fe(CO)C(O)Me](\mu\text{-}\eta^1\text{:}\ \eta^1\text{-dppe})[(4\text{-exo-}MeC_5H_5)Fe(CO)_2]$, Organometallics 14 (1995) 1514–1517.
[43] H.B. Kwon, Reaction of Methyl-$Fe(\eta^5\text{-}C_5H_5)(CO)_2$ with 1,2-Bis(diphenylphosphino) ethane, J. Korean Chem. Soc. 45 (1) (2001) 90–91.
[44] Similar migratory insertion reactions promoted by diphosphines generating bimetallic diiron systems have been reported: M. Kumar, A. Metta-Magana, H.K. Sharma, K.H. Pannell, Phosphine induced migratory CO insertion into the Fe–CH2 bond of the organometallic polymer-$[(\eta^5\text{-}C_5H_4)Fe(CO)_2\ CH_2SiMe_2]_n$-and characterization of model iron complexes, Dalton Trans. 39 (2010) 7125–7131.
[45] U. Knof, A. von Zelewsky, Predetermined chirality at metal centres, Angew. Chem. Int. Ed. 38 (3) (1999) 302–322.
[46] M. Timm, L. Saaby, L. Moesby, E.W. Hansen, Considerations regarding use of solvents in in vitro cell based assays, Cytotechnology 65 (5) (2013) 887–894.
[47] (a) A plethora of μ-phosphane bridged diiron complexes exist. See as selected examples: Q.-L. Li, S. Lu, R.-F. Zhang, D. Zhao, C.-L. Ma, Substitution reactions of diiron diselenolato complex with bisphosphine ligands, Polyhedron 160 (2019) 255–260;
(b) A. Rahaman, S. Ghosh, S. Basak-Modi, A.F. Abdel-Magied, S.E. Kabir, M. Haukka, M.G. Richmond, G.C. Lisensky, E. Nordlander, G. Hogarth, Chalcogenide-capped triiron clusters $[Fe_3(CO)_9(\mu_3\text{-}E)_2]$, $[Fe_3(CO)_7(\mu_3\text{-}CO)(\mu_3\text{-}E)(\mu\text{-dppm})]$ and $[Fe_3(CO)_7(\mu_3\text{-}E)_2(\mu\text{-dppm})]$ (E = S, Se) as proton-reduction catalysts, J. Organ. Chem. 880 (2019) 213–222;
(c) S. Ghosh, B.E. Sanchez, I. Richards, M.N. Haque, K.B. Holt, M.G. Richmond, G. Hogarth, Biomimetics of the [FeFe]-hydrogenase enzyme: Identification of kinetically favoured apical-basal $[Fe_2(CO)_4(\mu\text{-}H)\{\kappa2\text{-}Ph_2PC(Me_2)PPh_2\}(\mu\text{-pdt})]^+$ as a proton-reduction catalyst, J. Organm. Chem. 812 (2016) 247–258;
(d) M. Kaiser, G. Knoer, Synthesis, Characterization, and reactivity of functionalized trinuclear iron-sulfur clusters – a new class of bioinspired hydrogenase models, Eur. J. Inorganic Chem. 2015 (2015) 4199–4206;
(e) F.I. Adam, G. Hogarth, S.E. Kabir, I. Richards, Models of the iron-only hydrogenase: Synthesis and protonation of bridge and chelate complexes $[Fe_2(CO)_4\{Ph_2P(CH_2)_nPPh_2\}(\mu\text{-pdt})]$ (n =2-4) - evidence for a terminal hydride intermediate, Comp. Rendus Chemie 11 (2008) 890–905;
(f) S. Ezzaher, J.-F. Capon, F. Gloaguen, F.Y. Petillon, P. Schollhammer, J. Talarmin, Electron-transfer-catalyzed rearrangement of unsymmetrically substituted diiron dithiolate complexes related to the active site of the [FeFe]-hydrogenases, Inorganic Chem. 46 (2007) 9863–9872;
(g) Z.-F. Meng, H.-L. Gao, J.-X. Wang, J.-Y. Shang, C.-G. Li, Phenyl-functionalized diiron propanediselenolato complexes containing the chelated or bridged 1,3-bis (diphenylphosphine)propane ligand, J. Coordination Chem. 71 (2018) 2953–2964;
(h) G.-R. Xu, L. Liu, H.-L. Gao, J.-Y. Shang, C.-G. Li, Phenyl-functionalized diiron propane diselenolato complexes containing intramolecular bridging diphosphine ligands, J. Coord. Chem. 70 (2017) 2684–2694.
[48] T. Mosmann, Rapid colorimetric assay for cellular growth and survival: application to proliferation and cytotoxicity assays, J. Immunol. Methods 65 (1983) 55–63.

[49] Gaussian 09, Revision A.02, M.J. Frisch, G.W. Trucks, H.B. Schlegel, G.E. Scuseria, M.A. Robb, J.R. Cheeseman, G. Scalmani, V. Barone, G.A. Petersson, H. Nakatsuji, X. Li, M. Caricato, A. Marenich, J. Bloino, B.G. Janesko, R. Gomperts, B. Mennucci, H.P. Hratchian, J.V. Ortiz, A.F. Izmaylov, J.L. Sonnenberg, D. Williams-Young, F. Ding, F. Lipparini, F. Egidi, J. Goings, B. Peng, A. Petrone, T. Henderson, D. Ranasinghe, V.G. Zakrzewski, J. Gao, N. Rega, G. Zheng, W. Liang, M. Hada, M. Ehara, K. Toyota, R. Fukuda, J. Hasegawa, M. Ishida, T. Nakajima, Y. Honda, O. Kitao, H. Nakai, T. Vreven, K. Throssell, J. A. Montgomery, Jr., J.E. Peralta, F. Ogliaro, M. Bearpark, J.J. Heyd, E. Brothers, K.N. Kudin, V.N. Staroverov, T. Keith, R. Kobayashi, J. Normand, K. Raghavachari, A. Rendell, J.C. Burant, S.S. Iyengar, J. Tomasi, M. Cossi, J.M. Millam, M. Klene, C. Adamo, R. Cammi, J.W. Ochterski, R.L. Martin, K. Morokuma, O. Farkas, J.B. Foresman, D.J. Fox, Gaussian, Inc., Wallingford, CT, 2016.